Dynamic Range Performance of a MOS Active Attenuator

Kou-Hung Loh
Department of Electrical Engineering
Texas A&M University
College Station, Texas 77843

Randall L. Geiger
Department of Electrical and Computer Engineering
Iowa State University
Ames, Iowa 50011-3060

Abstract

The dynamic range performance of an active MOS attenuator circuit suitable for analog monolithic applications is presented. The attenuator exhibits low input referred noise. An application using the active attenuator as the input stage of a transconductance amplifier is discussed. Tradeoffs between power consumption, circuit area, attenuation ratio and dynamic range are considered.

Introduction

Attenuators are useful in many discrete as well as integrated circuits. One application involves preceeding the input stage of CMOS transconductance amplifiers (TAs) with an attenuator to improve the signal handling capabilities [1-2]. In this paper, the operation principle and noise analysis of a simple linear attenuator consisting of two MOS transistors is presented. The dynamic range performance of attenuator-based TAs is discussed and compared with TAs without attenuators.

A MOS Active Attenuator

An active attenuator consisting of two n-channel MOSFETs is shown in Fig.1 [1]. The circuit is designed to operate with transistor M_2 in the ohmic region and transistor M_1 in the saturation region. Separate P–wells are used for M_1 and M_2 to enable matching of threshold voltages. It can be readily seen that M_1 and M_2 will be operating in the required region provided

$$V_{SS} + V_{T2} < V_i < V_{DD} + V_{T1} \tag{1}$$

where V_{T1} and V_{T2} are the threshold voltages of M_1 and M_2, respectively. If $V_{T1} = V_{T2}$, the relationship between V_o and V_i becomes linear. Equating the drain currents of M_1 and M_2 and setting $V_{T1} = V_{T2} = V_{TN}$, we obtain the linear relationship

$$V_o = \eta V_i + V_{SS}(1-\eta) - \eta V_{TN} \tag{2}$$

where η is the attenuation factor which is defined by

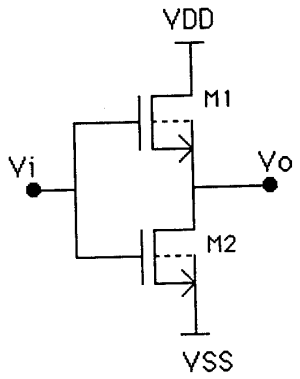

Fig.1 Schematics of an NMOS Active Attenuator

$$\eta = 1 - \frac{1}{\sqrt{1 + \frac{W_1 L_2}{W_2 L_1}}} \tag{3}$$

If mismatch effects in V_{T1} and V_{T2} are included, nonlinearities are only introduced through second-order effects involving the term $(V_{T1} - V_{T2})^2$ which will generally be very small. Threshold mismatches also introduce an additional small dc offset between V_o and V_i.

Noise Analysis

An equivalent circuit of the active attenuator based upon noiseless transistors and output noise sources is shown in Fig. 2. Since M_1 is operating in the saturation region and M_2 is in the ohmic region, the total thermal noise current spectral density at the output, S_{oT}, can be expressed by

$$S_{oT} = S_{o1T} + S_{o2T} = 4kT(\frac{2}{3}g_{m1} + \frac{1}{r_2}) \tag{4}$$

where S_{o1T} and S_{o2T} are the thermal current spectral densities of i_{n1} and i_{n2}, respectively, g_{m1} is the small signal transconductance of transistor M_1, and r_2 is the drain-to-source resistance of transistor M_2, defined respectively by

$$g_{m1} = \beta_1(V_{iQ} - V_{oQ} - V_{TN}) \tag{5}$$

CH 3006-4/91/0000 – 1733 $1.00 © IEEE

and

$$r_2 = [\beta_2(V_{iQ} - V_{SS} - V_{TN} - (V_{oQ} - V_{SS}))]^{-1} \quad (6)$$

where $\beta_1 = \mu C_{ox}(W_1/L_1)$ and $\beta_2 = \mu C_{ox}(W_2/L_2)$. It follows from (3), (5) and (6) that (4) can be rewritten as

$$S_{oT} = 4kT(V_{iQ} - V_{SS} - V_{TN})(1-\eta)(\frac{2}{3}\beta_1 + \beta_2) \quad (7)$$

Another noise source which plays an important role at lower/medium frequencies is the $1/f$ noise. The total $1/f$ noise current spectral density at the output is given by

$$S_{oF} = K_f\mu(\frac{1}{L_1^2} + \frac{1}{L_2^2})\frac{\beta_1\beta_2}{(\beta_1+\beta_2)}(V_{iQ} - V_{SS} - V_{TN})^2\frac{1}{f} \quad (8)$$

where K_f is the process dependent flicker noise factor. The total output noise voltage spectral density can be obtained by multiplying the output noise current density with the output resistance given by

$$r_o = r_2||(\frac{1}{g_{m1}}) = \frac{1}{(\beta_1+\beta_2)(1-\eta)(V_i - V_{SS} - V_{TN})} \quad (9)$$

From (3), (7), (8) and (9) the total noise spectral density at the output, S_{vo}, is given by

$$S_{vo} = \frac{4kT(\frac{2}{3}\beta_1 + \beta_2)}{(\beta_1+\beta_2)^2(1-\eta)(V_i - V_{SS} - V_{TN})}$$
$$+\frac{K_f}{C_{ox}}\eta^2(2-\eta)^2(\frac{L_1}{W_1L_2^2} + \frac{1}{W_1L_1})\frac{1}{f} \quad (10)$$

The total input referred noise spectral density of the attenuator can be obtained by dividing S_{vo} with η^2, i.e.,

$$S_{vi} = \frac{S_{vo}}{\eta^2} \quad (11)$$

For given η and L_2, S_{vi} can be minimized by setting $L_1 = L_2$, then from (10) and (11) the expression of the input referred noise spectral denisity, S_{vi}, of the active attenuator is given by

$$S_{vi} = \frac{4kT(\frac{2}{3}\beta_1 + \beta_2)}{\eta^2(\beta_1+\beta_2)^2(1-\eta)(V_i - V_{SS} - V_{TN})}$$
$$+\frac{2K_f}{C_{ox}}(2-\eta)^2\frac{1}{W_1L_1}\frac{1}{f} \quad (12)$$

For $V_{iQ} = 0V$, $\frac{\beta_1}{\beta_2} = \frac{1}{6}$, $(W_1/L_1) = 4/3$, η can be calculated to be $\frac{1}{13.48}$. Using the MOSIS 3μ paramters and setting $V_{DD} = -V_{SS} = 5V$, an output thermal noise density of $3.8nV/\sqrt{Hz}$ is obtained. This value is well below the input referred noise incurred by normal-size MOS transistors. In addition, the $\frac{1}{f}$ noise term in (12) also shows that the output $\frac{1}{f}$ noise can be much smaller than the input referred $\frac{1}{f}$ noise of normal MOS transistors if $\frac{1}{\eta}$ is large enough. These observations are encouraging in the sense that using such an attenuator as a signal front end is possible with little deterioration on the overall noise performance.

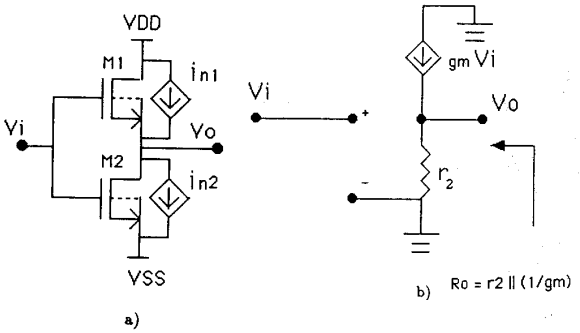

Fig.2 a) The Active Attenuator based upon Noiseless Transistors and Output Noise Current Sources b) The Small Signal Output Resistance of the Active Attenuator

Dynamic Range Analysis for Attenuator–Based TA Structure

In this section, the dynamic range performance of a simple TA structure is compared with that of an attenuator-based TA. It is assumed that the differential-pair input stage is the major noise and nonlinearity contributor in both TA structures. A simple single-ended TA consisting of a differential input transconductance stage and three current mirrors is shown in Fig.3. To obtain the dynamic range, both the signal swing at a given THD and the equivalent input referred noise voltage are needed. The differential output current, i_d, can be characterized by the equation

$$i_d = M_c g_{md} v_d \sqrt{1 - \frac{\beta_d v_d^2}{4I_{tail}}} \quad (13)$$

where M_c is the current mirror gain, $\beta_d = \mu C_{ox}(W_d/L_d)$ is the transconductance factor of the input transistors, and g_{md} is the transconductance of the input transistors given by

$$g_{md} = \beta_d V_{EB} \quad (14)$$

where $V_{EB} = (V_{GSQ} - V_T)$ denotes the excess bias voltage of the input transistors. If $\frac{\beta_d v_d^2}{4I_{tail}} << 1$, the following approximation can be made from (13)

$$i_d \approx M_c g_{md} v_d (1 - \frac{\beta_d v_d^2}{8I_{tail}}) \quad (15)$$

To obtain the total harmonic distortion (THD) at the output, consider a sinusoidal input signal

$$v_d = V_m cos(\omega_0 t) \quad (16)$$

By basic trignometry, we have

$$i_d \approx M_c g_{md} V_m [cos(\omega_0 t)(1 - \frac{3}{32V_{EB}}V_m^2)$$

$$-cos(3\omega_0 t)(\frac{1}{32V_{EB}}V_m^2)] \quad (17)$$

The THD can thus be approximated by

$$THD \approx \frac{1}{32}\frac{V_m^2}{V_{EB}} \quad (18)$$

The third harmonic dominates the THD of a simple differential pair. We define V_{max} as the maximum RMS input signal amplitude that can be applied without exceeding 1% THD at the output, V_{max} can be readily attainable from (18) giving

$$V_{max} = 0.4V_{EB} \quad (19)$$

For a simple TA structure, the input referred noise spectral density is given by

$$S_v = 2(\frac{8}{3}kT\frac{1}{g_{md}} + \frac{K_f}{C_{ox}W_dL_df}) \quad (20)$$

The total input referred RMS noise voltage, v_{ni}, can be obtained by integrating the noise spectral density over the passband, $f_l \leq f \leq f_r$, to obtain

$$v_{ni} = \sqrt{\frac{8}{3}kT\frac{2}{\beta_d V_{EB}}(f_r - f_l) + \frac{2K_f\mu}{\beta_d L_d^2}ln\frac{f_r}{f_l}} \quad (21)$$

If the dynmaic range is defined to be the ratio of V_{max} to v_{ni}, then for low-frequency passbands the dynamic range can be approximated by

$$DR \approx 0.4V_{EB}\beta_d^{\frac{1}{2}}L_d^2\sqrt{\frac{1}{ln\frac{f_r}{f_l}2K_f\mu}} \quad (22)$$

If the passband spreads over high frequencies, the following approximation can be used

$$DR \approx \frac{0.4V_{EB}^{\frac{3}{2}}\beta_d^{\frac{1}{2}}}{\sqrt{\frac{16}{3}kT(f_r - f_l)}} \quad (23)$$

Similar analysis can be performed to derive the dynamic range of an attenuator- based TA structure. As shown in Fig. 4, the differential input signal is attenuated by a factor η before applying to the differential-pair input stage. The output current can be characterized by

$$i_d = \eta M_c g_{md} v_d \sqrt{1 - \frac{\beta_d \eta^2 v_d^2}{4I_{tail}}} \quad (24)$$

Assuming all distortion is due to the differential input stage, the following equations can thus be derived:

$$THD = \frac{1}{32}\frac{\eta^2 V_m^2}{{V_{EB}}^2} \quad (25)$$

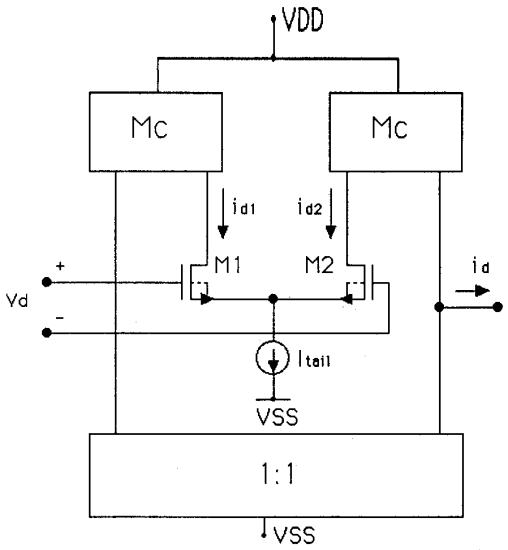

Fig.3 A Simple 3-Mirror TA Structure

and

$$V_{max} = 0.4\frac{V_{EB}}{\eta} \quad (26)$$

where V_{max} is the maximum RMS input voltage causing at most 1% THD at the output. The input referred noise voltage spectral density can be expressed by

$$S_v = 2(S_{v(att)} + \frac{S_{v(diff)}}{\eta^2}) \quad (27)$$

where $S_{v(att)}$ and $S_{v(diff)}$ represent the input referred noise spectral densities of the attenuator and the differential pair, respectively. From (27) we observe the later noise sources are "amplified" by a factor of $\frac{1}{\eta^2}$. It can be readily shown that S_v is dominated by the noise of the differential pair. The dynamic range of the attenuated TA structure is given by

$$DR \approx \frac{0.4V_{EB}}{v_{n(diff)}} \quad (28)$$

where $v_{n(diff)}$ is the total input referred RMS noise voltage in the passband. From (28) it is readily obtainable that the dynamic range of the attenuated TA structure can also be approximated by (22) and (23) at lower and higher frequencies, respectively.

To compare the two TA structures of Fig.3 and Fig.4, we will denote all parameters associated with simple TA structure with subscript 1 and denote attenuated TA parameters with subscript 2. The overall transconductance gains of the two circuits can thus be represented, respectively, by

$$g_{m1} = M_{c1}g_{md1} = M_{c1}\beta_{d1}V_{EB1} \quad (29)$$

and

$$g_{m2} = \eta M_{c2} g_{md2} = \eta M_{c2} \beta_{d2} V_{EB2} \tag{30}$$

If only white noise is considered, we can derive the following relationship from (23), (29) and (30):

$$\frac{DR_2}{DR_1} = \frac{V_{EB1}}{V_{EB2}} \sqrt{\frac{g_{m2} M_{c1}}{\eta g_{m1} M_{c2}}} \tag{31}$$

Similarly, from (22), (29) and (30) we can derive the dynamic range relationships for low-frequency approximation

$$\frac{DR_2}{DR_1} = \sqrt{\frac{V_{EB1}}{V_{EB2}}} \sqrt{\frac{g_{m2} M_{c1}}{\eta g_{m1} M_{c2}}} \tag{32}$$

For a given overall transconductance gain and a given excess bias voltage, it follows from (31) and (32) that the dynamic range of an attenuated TA structure can be improved by a factor of $\sqrt{\frac{1}{\eta}}$ if the current mirror gain remains constant. An alternative comparison is made for evaluating the TA structures based upon the same power consumption. If we assume the attenuators consume negligible power, then the power consumption for both structures can be approximated by

$$P \approx (V_{DD} - V_{SS}) \beta_d V_{EB}^2 (1 + M_c) \tag{33}$$

From (23), (29) and (33), we can express the dynamic range at higher frequencies for the simple TA structure in terms of the transconductance, mirror gain and power dissipation by

$$DR_1 \approx \frac{0.75 P_1}{(\frac{1}{\sqrt{M_{c1}}} + \sqrt{M_{c1}}) \sqrt{(f_r - f_l) g_{m1}} kT (V_{DD} - V_{SS})} \tag{34}$$

and for the attenuated TA, from (23), (30), and (33) by

$$DR_2 \approx \frac{\sqrt{\eta} 0.75 P_2}{(\frac{1}{\sqrt{M_{c2}}} + \sqrt{M_{c2}}) \sqrt{(f_r - f_l) g_{m2}} kT (V_{DD} - V_{SS})} \tag{35}$$

For the flicker-noise dominated approximation, we correspondingly have

$$DR_1 \approx \frac{0.4 L_{d1} \sqrt{P_1}}{\sqrt{2 \mu K_f (ln \frac{f_r}{f_l}) (V_{DD} - V_{SS}) (1 + M_{c1})}} \tag{36}$$

and

$$DR_2 \approx \frac{0.4 L_{d2} \sqrt{P_2}}{\sqrt{2 \mu K_f (ln \frac{f_r}{f_l}) (V_{DD} - V_{SS}) (1 + M_{c2})}} \tag{37}$$

For a given transconductance gain and a given power consumption, it follows directly from (34) and (35) that a unity mirror gain maximizes dynamic ranges. We can thus observe the dynamic range of the attenuated TA is reduced by $\sqrt{\eta}$ if the dynamic range is dominated by white noise. For the low-frequency approxmiation, as shown in (36) and (37), both structures exhibit similar dynamic range performance.

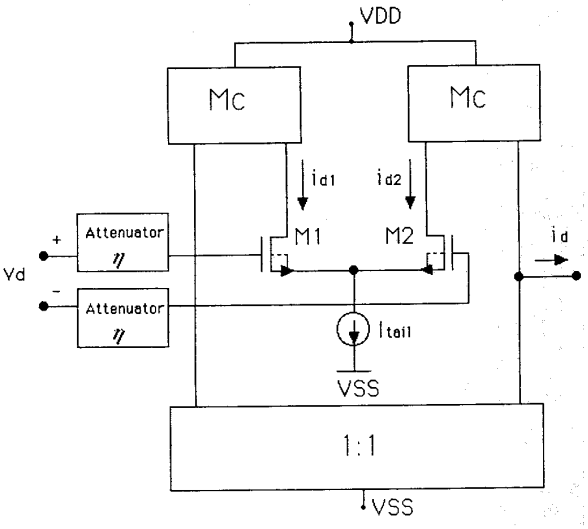

Fig.4 An Attenuator-based 3-Mirror TA Structure

Several conclusions may be drawn at this point. First, when a constant excess bias and a constant mirror gain are assumed for both TA structures, the dynamic range of the attenuated TA is improved to $\sqrt{\frac{1}{\eta}}$ times that of the simple TA with tradeoffs of larger power consumption and larger circuit area. The maximum input signal swing at 1% THD for the attenuated TA can be improved by $\frac{1}{\eta}$. The structure is especially useful when large signal handling capability is required. When constant power is assumed for both TA structures, the attenuated TA really has a deterioration in dynamic range over the simple TA structure at high frequencies where the noise characteristics are white noise dominated. Moreover, Biasing the attenuated TA for constant-power comparison becomes problematic for large attenuations because the excess bias for the differential pair becomes reduced driving the devices into weak inversion.

Conclusions

It has been shown that a simple two transistor active attenuator has a low input referred noise voltage. Applications of this attenuator as the front end of a transconductance amplifier which exhibits improved signal handling capability and reasonable dynamic range performance have been discussed.

References

[1] M. Van Horn and R.L. Geiger, "CMOS OTA Structure for Voltage-Controlled Analog Signal Processing", *Proc. 28th Midwest Symposium on Circuits and Systems*, pp596-599, Louisville, Kentucky, August 1985

[2] "LM13600/LM13600A/LM11600 Dual Operational Transconductance Amplifiers with Linearizing Diodes and Buffers", *Linear Databook, National Semiconductor* , 1986